



On the Cable Theory of Nerve Conduction

ICHIJI TASAKI*

STBB, LIMB, NICHD and LCMR, NIMH,

National Institutes of Health,

Bldg 13, Rm 3E-25,

Bethesda, MD 20892,

U.S.A.

E-mail: itasaki@erols.com

GEN MATSUMOTO

Brainway Group,

Brain Science Institute,

Riken, Wako,

Saitama 351-0198,

Japan

Conduction of an impulse in the nonmyelinated nerve fiber is treated quantitatively by considering it as a direct consequence of the coexistence of two structurally distinct regions, resting and active, in the fiber. The profile of the electrical potential change induced in the vicinity of the boundary between the two regions is analyzed by using the cable equations. Simple mathematical formulae relating the conduction velocity to the electrical parameters of the fiber are derived from the symmetry of the potential profile at the boundary. The factors that determine the conduction velocity in the myelinated nerve fiber are reexamined.

Published by Elsevier Science Ltd on behalf of Society for Mathematical Biology.

1. INTRODUCTION

The process of nerve conduction has been extensively studied in the past, both experimentally and theoretically. Mathematical theories of nerve conduction based on the modern cable concept were developed a long time ago by Offner *et al.* (1940), somewhat later by Rushton (1951), and eventually by Hodgkin and Huxley (1952). Nevertheless, in view of the fact that the nature of the rapid structural changes in the nerve fiber associated with nerve conduction has been elucidated only in recent years [see Tasaki (1999a,b) and Tasaki (2002)], it is deemed worthwhile to reexamine the process of nerve conduction.

The classic papers published by Cole and Curtis (1939), by Cole and Hodgkin (1939) and by Hodgkin and Rushton (1946), describing the basic cable properties

*Author to whom correspondence should be addressed.

of the invertebrate giant axon, provide the starting point of the present mathematical analysis. The process of nerve conduction is analyzed by incorporating the electrical manifestations of the discrete structural change in the axon membrane into the cable-like electrical network representing the properties of the axon. The interaction between the active and resting regions of the axon, by virtue of the 'local current' (Hermann, 1879), assumes the crucial role in the nerve conduction process.

The present analysis of the conduction velocity is an extension of the studies published previously by Matsumoto and Tasaki (1977) and by Tasaki (2002). It should be remarked that, in these studies, the behavior of the nerve fiber is described in terms of coarse-grained variables without reference to the microscopic details of the membrane structure. No precise knowledge of the electrochemical processes serving to maintain the membrane emf and resistivity is required in the present analysis.

2. POTENTIAL PROFILE IN THE VICINITY OF THE BOUNDARY BETWEEN THE ACTIVE AND RESTING REGIONS

Let us consider the process of nerve conduction taking place in a nonmyelinated nerve fiber placed in a large volume of saline solution. To dispel the chemical and thermodynamic uncertainties encountered in studies of intact (metabolizing) nerve fibers, a squid giant axon internally perfused with a 400 meq l⁻¹ K⁺-salt solution and immersed in artificial sea-water is considered initially. An axon carrying a nerve impulse is visualized as a thin, cylindrical layer of macromolecular material, enclosed in a superficial layer, known as 'axolemma-ectoplasm complex' (Metuzals *et al.*, 1981) and designated in this paper simply as 'membrane', which consists of two structurally distinct regions, active and resting. The boundary between the two regions is moving along the axon at a constant velocity.

The electrical properties of the axon are represented by the network illustrated in Fig. 1. In the resting state, the potential inside the axon (referred to as the potential outside) at position x along the axon at time t , $V(x, t)$, satisfies

$$c_m \frac{\partial V}{\partial t} + \frac{1}{r_m} (V - E_r) = \frac{1}{r_i} \frac{\partial^2 V}{\partial x^2}, \quad (1)$$

where c_m is the membrane capacitance, r_m the membrane resistance, E_r the emf of the membrane and r_i is the longitudinal resistance of the axon in the resting state (see Fig. 1, right). Equation (1) states that the membrane current, consisting of the capacitive and ohmic components, is directly related to the second derivative of the potential, $\partial^2 V / \partial x^2$, by way of conductivity of the axon interior, $1/r_i$.

Analogously, the equation describing the behavior of the active region of the axon is

$$c_m^* \frac{\partial V}{\partial t} - \frac{1}{r_m^*} (E_a - V) = \frac{1}{r_i} \frac{\partial^2 V}{\partial x^2}, \quad (2)$$

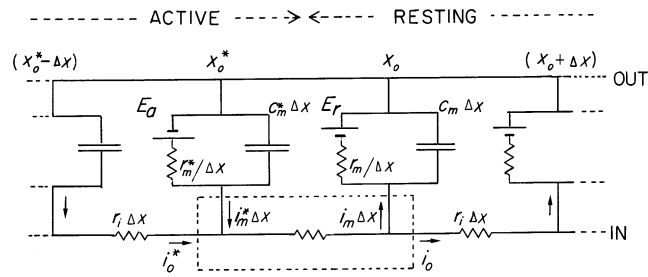


Figure 1. Electrical network used for explaining the process of nerve conduction in a squid giant axon. The diagram illustrates the electrical properties of the axon membrane in the vicinity of the boundary between the resting and active regions. The symbol $r_m/\Delta X$ represents the resistance of the element of the membrane of ΔX in length in the resting state. Other symbols are explained in the text. The symbols marked with asterisk indicate the quantities representing the properties of the axon membrane in the active state.

where c_m^* , r_m^* and E_a are the membrane capacitance, resistance and emf in the active region of the axon, respectively (see Fig. 1, left).

Suppose that the nerve impulse is propagating in the positive direction of x at a constant velocity v . To an observer moving along with the propagating impulse, the position of the boundary between the resting and active regions remains stationary and the potential profile seen in the vicinity of the boundary is time-independent. To analyze the potential profile in the vicinity of the boundary, therefore, it is convenient to adopt a new space variable X defined by $X \equiv (x - vt)$. When this variable is adopted, the partial differential equation (1) is reduced to the following ordinary differential equation

$$\frac{1}{r_i} \frac{d^2 V}{dX^2} + c_m v \frac{dV}{dX} - \frac{1}{r_m} (V - E_r) = 0. \tag{3}$$

The solution of this equation is found to be

$$V = E_r + (V_o - E_r) e^{-(X - X_o)\xi}, \tag{4}$$

where V_o is the potential at the receding end of the resting region, $X = X_o$, and ξ is the solution of the quadratic equation

$$\frac{1}{r_i} \xi^2 - c_m v \xi - \frac{1}{r_m} = 0. \tag{5}$$

The physiologically meaningful solution of equation (5) is

$$\xi = \frac{c_m v + \sqrt{(c_m v)^2 + 4/(r_i r_m)}}{2/r_i}. \tag{6}$$

The corresponding equations for the active region are

$$\frac{1}{r_i} \frac{d^2 V}{dX^2} + c_m^* v \frac{dV}{dX} + \frac{1}{r_m^*} (E_a - V) = 0 \quad (7)$$

and

$$V = E_a - (E_a - V_o^*) e^{-(X_o^* - X)\eta}, \quad (8)$$

where V_o^* is the potential at the advancing end of the active region (where $X = X_o^*$), and η is the solution of the quadratic equation

$$\frac{1}{r_i} \eta^2 + c_m^* v \eta - \frac{1}{r_m^*} = 0. \quad (9)$$

The meaningful solution in this case is:

$$\eta = \frac{-c_m^* v + \sqrt{(c_m^* v)^2 + 4/(r_i r_m^*)}}{2/r_i}. \quad (10)$$

Note that the active region extends formally from $-\infty$ to X_o^* .

It is seen in Fig. 1 that, in the vicinity of the boundary, there is an inwardly directed membrane current in the active region and an outwardly directed current in the resting region. The potential changes associated with the spread of these 'local currents' decays exponentially with increasing distance from the boundary. It is to be noted that $1/\eta$ and $1/\xi$, which are termed 'space parameters', measure the length scale of the potential spread.

In Fig. 1, we note that the advancing end of the active region is connected to the receding end of the resting state with a longitudinal electrical resistance $(X_o^* - X_o)r_l$. This longitudinal resistance is traversed by the current that flows between the active and resting ends of the network. The potential drop across this resistance divided by $(X_o^* - X_o)$ gives the potential gradients, dV/dX , at the ends of both active and resting regions. Thus, from equations (4) and (8), we have

$$\xi(V_o - E_r) = \eta(E_a - V_o^*). \quad (11)$$

We note, in the network illustrated in Fig. 1, further that the algebraic sum of the currents passing through the closed surface indicated by the stippled rectangle at the boundary in the figure is equal to zero. (Note that the space enclosed by the surface corresponds to the interior of the axon occupied by the internal perfusion solution.) The difference Δi between the two longitudinal currents traversing the surface is given by

$$\Delta i = i_o^* - i_o = \frac{V(X_o^* - \Delta X) - V(X_o^*)}{r_i \Delta X} - \frac{V(X_o) - V(X_o + \Delta X)}{r_i \Delta X}$$

$$\begin{aligned}
 &= \frac{1}{2r_i} \left[\left. \frac{d^2V}{dX^2} \right|_{X_o^*} + \left. \frac{d^2V}{dX^2} \right|_{X_o} \right] \Delta X - O((\Delta X)^2) \\
 &= \left[-\frac{1}{2r_i} \eta^2 (E_a - V_o^*) + \frac{1}{2r_i} \xi^2 (V_o - E_r) \right] \Delta X - O((\Delta X)^2).
 \end{aligned}
 \tag{12}$$

The currents passing through the elements of the membrane, ΔX in length, located in the immediate vicinity of the boundary (see Fig. 1) are given by

$$i_m^* \Delta X = \left(-c_m^* \nu \eta + \frac{1}{r_m^*} \right) \Delta X (E_a - V_o^*) \tag{13}$$

and

$$i_m \Delta X = \left(c_m \nu \xi + \frac{1}{r_m} \right) \Delta X (V_o - E_r). \tag{14}$$

Thus, the requirement that $\Delta i + (i_m^* - i_m) \Delta X = 0$ leads to the following relation:

$$\left[-\frac{1}{2r_i} \eta^2 - c_m^* \nu \eta + \frac{1}{r_m^*} \right] (E_a - V_o^*) = \left[-\frac{1}{2r_i} \xi^2 + c_m \nu \xi + \frac{1}{r_m} \right] (V_o - E_r). \tag{15}$$

By use of equations (5) and (9), the sum of the terms inside the square bracket on the left and that on the right side of equation (15) are found to be equal to $\eta^2/(2r_i)$ and $\xi^2/(2r_i)$, respectively. Finally, from equation (11), we arrive at a very simple relation

$$\eta = \xi. \tag{16}$$

This is the condition that is fulfilled when the axon is carrying an impulse at a constant velocity ν . The potential profile seen under these conditions is illustrated in Fig. 2.

Every term on the right side of equations (6) and (10) is amenable to direct experimental determination. We have known for some time that the values of η and ξ calculated by using the observed values of r_m^* , c_m , ν , r_i etc. are actually very close to each other (Matsumoto and Tasaki, 1977). In the axon under consideration (diameter $d \approx 0.4$ mm and with 0.4 M K^+ -salt inside), the unit-area membrane resistance at the peak of excitation $R_m^* (= r_m^* \pi d)$ was approximately $22 \Omega \cdot \text{cm}^2$. The ratio r_m^*/r_m was roughly 0.01. The membrane capacitance per unit area $C (= c_m/\pi d \approx c_m^*/\pi d)$ is approximately $1 \mu\text{F cm}^{-2}$. The specific resistance $\rho (= r_i \pi d^2/4)$ of the 0.4 M K^+ -salt solution was $36 \Omega \text{ cm}$. The conduction velocity ν was 24 m s^{-1} . When these observed values are introduced into equations (6) and (10), it is found that both ξ and η are approximately $1/(1.1 \text{ mm})$.

The validity of equation (16) has been demonstrated further by a series of measurements in which the specific resistance of the internal K^+ -salt solution was systematically varied by successive dilution of the internal salt solution [see Table III in Matsumoto and Tasaki (1977)].

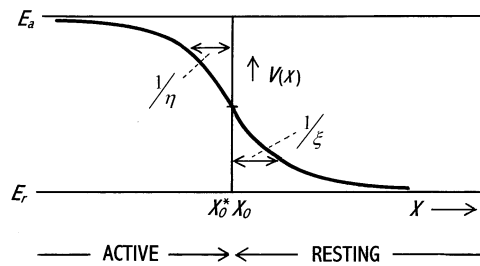


Figure 2. Diagrammatic representation of the potential profile in the vicinity of the boundary between the resting and active regions of a nonmyelinated nerve fiber. The ordinate portrays the electrical potential inside the axon, $V(X)$. The abscissa represents the distance along the axon from the boundary, X . In squid giant axons, $(E_a - E_r)$ is approximately 115 mV and the length $(\frac{1}{\xi} + \frac{1}{\eta})$ is roughly 2 mm. See the text.

3. DERIVATION OF THE CONDUCTION VELOCITY FORMULAE

We now derive, from the relation $\eta = \xi$, explicit formulae relating the conduction velocity to the electrical parameters of the axon. It follows from equations (6), (10) and (16) that

$$-c_m^*v + \sqrt{(c_m^*v)^2 + 4/(r_i r_m^*)} = c_m v + \sqrt{(c_m v)^2 + 4/(r_i r_m)}. \quad (17)$$

After some algebraic operation requiring repeated squaring, this equation gives

$$v = \sqrt{\frac{(1 - \kappa)^2}{(c_m + c_m^*)(c_m + \kappa c_m^*)r_i r_m^*}}, \quad (18)$$

where $\kappa = r_m^*/r_m$, namely, the ratio of the membrane resistance at the peak of excitation to that at rest. Since $\kappa \ll 1$ in normal squid giant axons, equation (18) reduces to

$$v \cong \frac{1}{\sqrt{(c_m + c_m^*)c_m r_i r_m^*}}. \quad (19)$$

When the change in the membrane capacitance during excitation is ignored, namely, when $c_m^* \cong c_m$, equation (19) becomes:

$$v \cong \frac{1}{c_m \sqrt{2r_i r_m^*}}, \quad (20a)$$

or

$$v \cong \frac{1}{\sqrt{8}} \frac{1}{C} \sqrt{\frac{d}{R^* \rho}}. \quad (20b)$$

This is the formula reported previously (Matsumoto and Tasaki, 1977), relating the conduction velocity v to C (membrane capacitance per unit area), d (diameter),

R^* (unit area membrane resistance to radial current at peak of excitation) and ρ (longitudinal specific resistance of the axon interior).

It is to be noted that the conduction velocity formulae described above do not explicitly contain $(E_a - E_r)$, i.e., the term representing the action potential amplitude. The reason for the absence of this term is that we have chosen, at the outset of the present analysis, only those axons capable of carrying an impulse at a constant velocity. Obviously, there is an implicit assumption as to the acceptable range of $(E_a - E_r)$ in the present analysis (see below).

The above-cited equations indicate a strong dependence of the conduction velocity on the membrane capacity. Since the capacity is considered to be determined by the polarizability of the strands of polyelectrolyte molecules in the 'membrane' and since the polarizability of anionic polyelectrolytes is known to be strongly affected by the Ca^{2+} - Na^+ concentration ratio in the medium [see Minakata (1972)], a significant increase in the membrane capacity is expected at the onset of a nerve impulse. However, the increase reported by Takashima (1979) was only about 20%. It is noted that the polyelectrolyte strands in the superficial layer of a freshly isolated squid axon (excitable) are oriented predominantly in the longitudinal direction, i.e., in the direction parallel to the axon surface (Tasaki, 1999b). It appears that the structural change taking place at the onset of an impulse does not bring about a large change in the membrane polarizability in the direction normal to the axon surface.

The dependence of the conduction velocity on the membrane resistance is quite significant. Obviously, no nerve conduction is expected when κ in equation (18) approaches unity, namely, when there is no significant change in the membrane resistance at the peak of excitation. When $\kappa \ll 1$, the velocity is expected to be inversely proportional to the square root of the membrane resistance at the peak of excitation, $\sqrt{R^*}$. The dependence of the velocity on the fiber diameter d is well known (Pumphrey and Young, 1938). The formulae described above are consistent with this known fact.

We now examine the validity of the simplified equation, equation (20b). In excised giant axons of the squid, C is about $1\mu\text{F cm}^{-2}$, R^* is $25 \sim 40 \Omega \cdot \text{cm}^2$, and ρ is $30 \sim 70 \Omega \cdot \text{cm}$ (Cole and Hodgkin, 1939; Hodgkin and Huxley, 1952). When these values are introduced into equation (20b), the conduction velocity v calculated for giant axons of 0.05 cm in diameter is found to be $15 \sim 28 \text{ m s}^{-1}$, with an average of 22 m s^{-1} . No adjustable parameters were used in this calculation. The agreement between the calculated and observed values is very good.

Squid giant axons which are internally perfused with a dilute Na^+ -salt solution and immersed in a Ca^{2+} -salt solution are known to sustain their ability to carry propagated impulses (Inoue *et al.*, 1974). It has been shown (Matsumoto and Tasaki, 1977) that the conduction velocities observed under these and other experimental conditions are in general agreement with the values calculated by use of equations (20).

4. PHYSIOLOGICAL SIGNIFICANCE OF THE SPACE PARAMETERS $1/\eta$ AND $1/\xi$

Figure 2 shows the spatial distribution of the potential change generated in the vicinity of the boundary between the active and resting regions of an axon carrying an impulse. The diagram in this figure illustrates the potential $V(X)$ at position X along the axon measured from the boundary which is moving at a constant velocity v . Since the length of the transitional zone intervening between the active and resting regions, $(X_o^* - X_o)$, is considered to be far smaller than the space parameters, the boundary between the two regions is indicated by a single vertical line in the middle of the diagram.

It is seen in the figure that the portion of the potential profile in the resting region [described by equation (4)] extends from the midpoint between the upper and lower limits of the potential, $V = \frac{1}{2}(E_a - E_r)$, toward the positive end of the axon. The portion of the profile in the active region [described by equation (8)] extends from the midpoint toward the negative end of the axon. From the equality of the space parameter $1/\xi$ of the resting region to that of the active region $1/\eta$ [equations (11) and (16)], it follows that the total potential profile is made up of two identical exponentials.

The numerical value of the parameter can be obtained, when v , r_m^* , etc. are known, directly from equations (6) and (10), or simply by the following equation

$$\frac{1}{\xi} = \frac{1}{\eta} = \sqrt{2r_m^*/r_i}, \quad (21)$$

which can be obtained by introducing v from equation (20a) into (6) or (10). As has been stated already, the space parameter is roughly 1 mm in squid axons of about 0.4 mm in diameter. [Note that this parameter, described by equation (21), is formally similar to the 'space constant' λ of an axon in the resting state, $\lambda = \sqrt{(r_m/r_i)}$, which is around 7 mm in these axons.]

Since the velocity v of the impulse propagating along the axon is chosen to be a constant, the spatial profile of the potential change can be converted into its temporal profile simply by dividing the coordinate X by $-v$. Therefore, the diagram in Fig. 2 indicates that the rising phase of a propagated action potential is also made up of two identical exponentials, symmetric with respect to the midpoint. This actually is a general feature of the propagated action potentials recorded from the interior of the freshly excised giant axons of the squid.

Interestingly, in their classical analysis of the time-course of the propagated action potential, Cole and Curtis pointed out that the rising phase of the recorded action potential is nearly symmetric with respect to the half-maximum point [see p. 664 in Cole and Curtis (1939)]. Furthermore, they noted that the onset of the abrupt fall in the membrane resistance (associated with ' $r_m \rightarrow r_m^*$ ' transition in the present analysis) coincides roughly with the time when the potential rises to

the half-maximum level (see p. 667). This characteristic of the propagated action potential is also properly represented in the diagram of Fig. 2.

In freshly excised axons, the threshold voltage level at which an action potential is evoked by a short current pulse is normally less than 25 mV ($\approx RT/F$ in electrochemistry) above the resting potential level, E_r . Since $(E_a - E_r)$ is approximately 115 mV, it is evident that the process underlying the propagation of a normal nerve impulse goes on with a considerable margin of safety. The active membrane element located at the advancing end of the active region delivers a strong, exponentially rising 'restimulating current' to the neighboring elements in the resting state. The rapidity of the ' $r_m \rightarrow r_m^*$ ' transition in the nerve fiber is believed to result from the high rate of rearrangement of water molecules around Ca-ions and flexible strands of the anionic macromolecules [cf. Levine and Williams (1982, p. 14)].

[No nerve conduction (at a constant velocity) is expected to take place when the action potential amplitude is reduced (e.g., by application of an anesthetic to the axon) to a level around twice the threshold potential.]

Now, it should be remarked that the electrical network representing the axon membrane in its resting state is assumed to be a simple *linear* network. In fact, it is known that, when the strength of the stimulating current is well below the threshold, the voltage developed across the membrane (in the resting state) varies linearly with the applied current (Hodgkin and Rushton, 1946; Tasaki, 1982). A deviation from the linearity is observed when the potential evoked approaches the threshold level; and this deviation is attributed to the intervention of a 'subthreshold response' (Hodgkin and Rushton, 1946). However, when the stimulating current is strong and the potential evoked quickly rises to a high level, as in the case of restimulation by the local current, there is no time for intervention of a subthreshold response and, consequently, the deviation from the linearity is negligibly small [see pp. 64 and 108 in Tasaki (1982)]. [Note that, in fresh squid axons, the time required for re-stimulation ($\approx 1/\xi v$) is about 50 μ s, which is far shorter than the duration of the action potential (~ 1 ms).]—It is known also that there is an approximately linear relationship between the voltage and current measured in the axon membrane in its active state [see e.g., Fig. 3, Matsumoto and Tasaki (1977)].

In the theory of propagation of the rising phase and peak of the action potential formulated by Hodgkin and Huxley, the conduction velocity is given by $v = [Kd/(4\rho C)]^{1/2}$, where the quantity K depends on the conductance $g_{Na}(V, t)$ in their theory in an intricate fashion [Hodgkin and Huxley (1952, p. 524, 528)]. When the quantity K is replaced simply with $1/(2R^*C)$, their velocity equation is converted to equation (20b).

5. A BRIEF ACCOUNT OF NERVE CONDUCTION IN MYELINATED FIBERS

The electrical network representing the properties of a myelinated nerve fiber is complicated by the existence of the myelin sheath which is interrupted by nodes

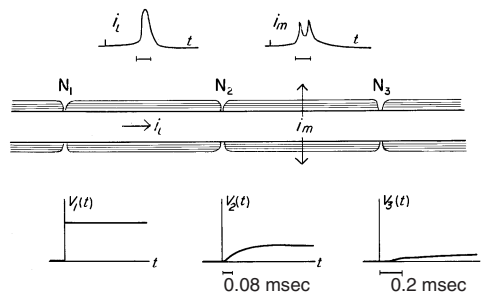


Figure 3. Top: tracings of the action currents recorded from the middle of an internode of a bull-frog motor nerve fiber. The left tracing is a copy of the longitudinal current; the right tracing, the current traversing the myelin sheath. The bars below the tracings represent the internodal conduction time. Middle: schematic diagram of a myelinated nerve fiber. Bottom: time-course of the voltage applied to the 'nodal membrane at node N_1 ' (left) and those of the voltage recorded across the 'nodal membrane at N_2 and N_3 ' (middle and right tracings). These records were taken from an electrical network analog (described in text). The bars below the middle and right tracings represent 0.08 and 0.2 ms, respectively.

of Ranvier at more-or-less regular intervals. Motor nerve fibers of the bull-frog are 12–15 μm in outside diameter and the internodal distance is 2–2.5 mm (Fig. 3). At the node of a freshly excised fiber, the axolemma surface (devoid of myelin covering) is roughly $0.5 \sim 1 \mu\text{m}$ wide. Since the conduction velocity in these fibers is $20 \sim 25 \text{ m s}^{-1}$, the internodal conduction time is roughly 0.1 ms [cf. Tasaki (1982)].

It is relatively easy to record the longitudinal current associated with a propagated impulse from the middle of the internode of a single motor nerve fiber (see tracing marked ' i_l ' in the figure). It is also possible to record the membrane current in the internodal region of a fiber (tracing ' i_m '). By analyzing the time-courses of these current records, the electrical parameters of the frog motor nerve fiber have been determined (Tasaki, 1955).

$$\begin{aligned}
 \text{Capacity of myelin sheath } (c_m): & 1.6 \times 10^{-11} \text{ F cm}^{-1} \\
 \text{Resistance of myelin sheath } (r_m): & 2.9 \times 10^7 \Omega \cdot \text{cm} \\
 \text{Capacity of nodal membrane } (C): & 1.5 \times 10^{-12} \text{ F} \\
 \text{Resistance of nodal membrane } (R): & 41 \times 10^6 \Omega \\
 \text{Resistance of axis cylinder } (r_i): & 1.45 \times 10^8 \Omega \text{ cm}^{-1}.
 \end{aligned}$$

These results indicate that the myelin sheath behaves like a leaky capacitor. It is to be noted that the capacity–resistance product, $c_m r_m$, of the myelin sheath is roughly 0.5 ms. In stimulation of a nerve fiber with long current pulses (> 1 ms duration), therefore, the myelin sheath can be treated as a good insulator, because the stimulating current goes in and out of the fiber mainly through the nodal membrane. However, when the stimulus duration becomes shorter than about 0.5 ms, the stimulating current is short-circuited by the capacitive flow of electricity through the myelin sheath. Consequently, the threshold strength of a stimulating pulse markedly rises when the duration is reduced beyond about 0.5 ms. In clas-

sical physiology, this dependence of threshold strength on the stimulus duration is known as the ‘strength-duration relation’ [see p. 95 in Tasaki (1982)].

The capacitive flow of electricity through the myelin sheath also plays a crucial role in the following analysis of the conduction velocity in the fiber. In the myelinated region of the fiber, the spread of the electrical potential inside the fiber, $V(x, t)$, may be described simply by

$$\frac{\partial V}{\partial t} = \frac{1}{c_m r_i} \frac{\partial^2 V}{\partial x^2}, \quad (22)$$

the coefficient $1/(c_m r_i)$ being about $430 \text{ cm}^2 \text{ s}^{-1}$ in frog motor nerve fibers. [Note that V in this and the following equations corresponds to $(V - E_r)$ in equation (1).] In a myelinated nerve fiber carrying an impulse, when one of the nodes, say N_1 , becomes active, the resulting rise of the potential inside the fiber spreads along the internode from N_1 toward its neighboring node, N_2 (see Fig. 3). At the time when the potential across the membrane at N_2 rises above the threshold level, node N_2 also becomes active. The internodal conduction time is determined primarily by the time required for the spread of the potential from one node of the fiber to the next.

When node N_2 is kept in its resting state, the distribution of the potential $V(x, t)$ and the longitudinal current $i_l(x, t)$ in the vicinity of active node N_1 can be described by the following solution of equation (22):

$$V = E_a \left\{ 1 - \operatorname{erf} \frac{x}{2\sqrt{t/(c_m r_i)}} \right\}, \quad (23)$$

and

$$i_l = \frac{1}{r_i} \frac{\partial V}{\partial x} = \frac{1}{r_i} \frac{E_a}{\sqrt{\pi t/(c_m r_i)}} e^{-x^2 c_m r_i / (4t)} \quad (24)$$

where E_a is the value of V across the membrane of N_1 located at $x = 0$ and ‘erf’ represents the error function solution [see p. 60 in Carslaw and Jaeger (1959)]. It is seen from these equations that the time t required for any point to reach a given potential (or current intensity) is proportional to the square of the distance x from the active node, N_1 . From equation (23), it is estimated that, at the distance of 2 mm from N_1 , the time required for the potential to rise to 1/2 of the final level is roughly 0.1 ms. (However, note that the singularity of the fiber at the nodes is ignored in this estimation.)

It is desirable to estimate the time-course of the potential reached in the interior of N_2 prior to the onset of the excitation process at this node. Anticipating some difficulty in the purely mathematical approach to this estimation, the following simple observations were made on an electrical network analog of the nerve fiber. This electrical network was fabricated using commercially available, small resistors and capacitors. It was made up of four ‘nodes’ separated by three ‘internodes’. In the network, the capacities were chosen to be 1000-times as large as those

of the real nerve fiber (listed above), and the resistances were reduced by a factor of 1/1000, keeping the capacity–resistance products unaltered. Each of the three ‘internodes’ was divided into 10 equivalent sections, replacing the continuously distributed capacity around the axis-cylinder with a finite number of capacitors. A rectangular voltage pulse was delivered directly to the ‘node’ N_1 at one end of the network, and the time-courses of the potentials developed at the neighboring ‘nodes’ N_2 and N_3 were recorded with an oscilloscope (see Fig. 3, bottom).

It is seen in the figure that the potential $V_2(t)$ reached at the next node (N_2) was slightly smaller than one-half of the potential delivered to N_1 . The time required to rise to 50% of the final level was about 0.08 ms. The potential $V_3(t)$ reached at N_3 was about 20% of the potential at N_1 , and the delay at the 50% level was about 0.2 ms. A ‘silent period’ of about 0.05 ms was observed between the onset of the potential at N_1 and that at N_3 .

Based on the results of these observations, it seems safe to conclude that a considerable portion of the internodal conduction time is attributable to the delay caused by the capacity of the myelin sheath. [See p. 99 in Tasaki (1982), for physiological data in support of this conclusion.] The action potential developed at one node of a fiber carrying an impulse is preceded, as in the case of nonmyelinated nerve fibers, by a small potential rise derived from the activity of the preceding node.

Finally, the process of nerve conduction in small myelinated nerve fibers is briefly discussed. From equations (23) and (24), it is seen that the time required for the potential to spread from one node to the next is governed primarily by the exponent $-x^2 c_m r_i / 4t$ in the equations. The longitudinal resistance (of the axis-cylinder) per unit length of the fiber, r_i , varies inversely with the square of the internal diameter d' of the myelin sheath. The capacitance of the myelin sheath, c_m , is determined by the ratio d/d' , where d is the external diameter of the myelin sheath; and it is known that this ratio does not vary appreciably with the fiber diameter [see Rushton (1951, p. 105)]. The internodal distance l varies directly with the diameter d (Tasaki *et al.*, 1943). Therefore, the value of $(l^2 c_m r_i)$ is not expected to change appreciably with d . Thus, the experimental fact that the internodal conduction time is nearly independent of the fiber diameter (Hursh, 1939; Tasaki *et al.*, 1943) can be explained on the same theoretical basis.

6. CONCLUSION

- (1) A nonmyelinated nerve fiber carrying an impulse is represented by a linear electrical network, consisting of two distinct regions, active and resting. ‘Local currents’ are generated in the vicinity of the boundary between the two regions. These currents, resulting from the difference in the membrane emf and resistance in the two regions, play a crucial role in the process of nerve conduction (Fig. 1).
- (2) The distribution of the potential associated with the ‘local currents’ is symmetric with respect to the boundary (moving at a constant velocity) between

the resting and active region (Fig. 2). A faithful reflection of this symmetry is seen in the rising phase of a propagated action potential.

- (3) Simple formulae [equations (18)–(20)] are derived relating the conduction velocity to the electrical parameters (membrane capacity, membrane resistance during excitation, and diameter) of the nonmyelinated nerve fiber.
- (4) It is emphasized that the internodal conduction time in the myelinated nerve fiber is governed primarily by the electrical capacity of the myelin sheath.

ACKNOWLEDGEMENTS

I express my gratitude to Dr Peter Bassler and Dr Ralph Nossal of the Laboratory of Integrative and Medical Biophysics, NICHD, for their continuous support.

REFERENCES

- Carslaw, H. S. and J. C. Jaeger (1959). *Conduction of Heat in Solids*, 2nd edn, Oxford: Clarendon Press.
- Cole, K. S. and H. J. Curtis (1939). Electric impedance of the squid giant axon during activity. *J. Gen. Physiol.* **22**, 649–670.
- Cole, K. S. and A. L. Hodgkin (1939). Membrane and protoplasm resistance in the squid giant axon. *J. Gen. Physiol.* **22**, 671–687.
- Hermann, L. (1879). *Allgemeine Nervenphysiologie*. Handbuch der Physiologie. Ister Theil. 1-196. F. C. W. Vogel, Leipzig.
- Hodgkin, A. L. and A. F. Huxley (1952). A quantitative description of membrane current and its application to conduction and excitation in nerve. *J. Physiol.* **117**, 500–544.
- Hodgkin, A. L. and W. A. H. Rushton (1946). The electrical constants of a crustacean nerve fibre. *Proc. R. Soc. London B* **133**, 444–479.
- Hursh, J. B. (1939). Conduction velocity and diameter of nerve fibers. *Am. J. Physiol.* **127**, 131–153.
- Inoue, I., I. Tasaki and Y. Kobatake (1974). A study of the effects of externally applied sodium ions and detection of spatially non-uniformity of the squid axon membrane under internal perfusion. *Biophys. Chem.* **2**, 116–126.
- Levine, B. A. and R. J. P. Williams (1982). The chemistry of calcium ion and its biological relevance, in *The Role of Calcium in Biological Systems*, Vol. 1, L. J. Anghileri and A. M. Tuffet-Anghileri (Eds), Boca Raton, FL: CRC Press, Inc., pp. 3–26.
- Matsumoto, G. and I. Tasaki (1977). A study of conduction velocity in nonmyelinated nerve fibers. *Biophys. J.* **20**, 1–13.
- Metuzals, J., I. Tasaki, S. Terakawa and D. F. Clapin (1981). Removal of the Schwann sheath from the giant nerve fiber of the squid: an electron-microscopic study of the axolemma and associated axoplasmic structures. *Cell Tissue Res.* **221**, 1–15.
- Minakata, A. (1972). Dielectric properties of polyelectrolytes. III. Effects of divalent cations on dielectric increments of polyacids. *Biopolymers* **11**, 1567–1581.

- Offner, F., A. Weinberg and G. Young (1940). Nerve conduction theory: some mathematical consequence of Bernstein's model. *Bull. Math. Biophys.* **2**, 89–103.
- Pumphrey, R. A. and J. Z. Young (1938). The rate of conduction of nerve fibres of various diameters in cephalopods. *J. Exp. Biol.* **15**, 453–466.
- Rushton, W. A. H. (1951). A theory of the effects of fibre size in medullated nerve. *J. Physiol.* **115**, 101–122.
- Takashima, S. (1979). Admittance change of squid axon during action potentials. *Biophys. J.* **26**, 133–142.
- Tasaki, I. (1955). New measurements of the capacity and the resistance of the myelin sheath and the nodal membrane of the isolated frog nerve fiber. *Am. J. Physiol.* **181**, 639–650.
- Tasaki, I. (1982). *Physiology and Electrochemistry of Nerve Fibers*, New York: Academic Press.
- Tasaki, I. (1999a). Evidence for phase transition in nerve fibers, cells and synapses. *Ferroelectrics* **220**, 305–316.
- Tasaki, I. (1999b). Rapid structural changes in nerve fibers and cells associated with their excitation processes. *Japan. J. Physiol.* **49**, 128–138.
- Tasaki, I. (2002). Spread of discrete structural changes in synthetic polyanionic gel: a model of propagation of a nerve impulse. *J. Theor. Biol.* to appear.
- Tasaki, I., F. Ishii and H. Ito (1943). On the relation between the conduction rate, fiber diameter and internodal distance of the medullated nerve fiber. *Japan. J. Med. Sci. III.* **9**, 189–199.

Received 12 February 2002 and accepted 1 August 2002